HHS Public Access

Author manuscript

Nat Microbiol. Author manuscript; available in PMC 2016 September 02.

Published in final edited form as:

Nat Microbiol. ; 1: 15005. doi:10.1038/nmicrobiol.2015.5.

Local and Global Consequences of Flow on Bacterial Quorum Sensing

Minyoung Kevin Kim[1], **Francois Ingremeau**[2], **Aishan Zhao**[1], **Bonnie L. Bassler**[3,4,*], and **Howard A. Stone**[2,*]

[1]Department of Chemistry, Princeton University, Princeton, NJ 08544.

[2]Department of Mechanical and Aerospace Engineering, Princeton University, Princeton, NJ 08544.

[3]Department of Molecular Biology, Princeton University, Princeton, NJ 08544.

[4]Howard Hughes Medical Institute, Chevy Chase, MD 20815.

Abstract

Bacteria use a chemical communication process called quorum sensing (QS) to control collective behaviours, such as pathogenesis and biofilm formation[1,2]. QS relies on the production, release, and group-wide detection of signal molecules called autoinducers. To date, studies of bacterial pathogenesis in well-mixed cultures have revealed virulence factors and the regulatory circuits controlling them, including the overarching role of QS[3]. Although flow is ubiquitous to nearly all living systems[4], much less explored is how QS influences pathogenic traits in scenarios that mimic host environments, for example, under fluid flow and in complex geometries. Previous studies have showed that sufficiently strong flow represses QS[5–7]. Nonetheless, it is not known how QS functions under constant or intermittent flow, how it varies within biofilms or as a function of position along a confined flow, or how surface topography (grooves, crevices, pores) influence QS-mediated communication. We explore these questions using two common pathogens *Staphylococcus aureus* and *Vibrio cholerae*. We identify conditions where flow represses QS and other conditions where QS is activated despite flow, including characterizing geometric and topographic features that influence the QS response. Our studies highlight that, under flow, genetically identical cells do not exhibit phenotypic uniformity with respect to QS in space and time, leading to complex patterns of pathogenesis and colonization. Understanding the ramifications of spatially and temporally non-uniform QS responses in realistic environments will be crucial for successful deployment of synthetic pro- and anti-QS strategies.

[*]**Corresponding authors:** bbassler@princeton.edu (B.L.B.) and hastone@princeton.edu (H.A.S.).

Supplementary Information is available.

The authors declare no competing financial interests.

Author Contributions M.K.K., F.I., B.L.B., and H.A.S. designed the experiments. M.K.K. and F.I. performed the experiments. A.Z. synthesized the AIP. F.I. constructed the quantitative model, and H.A.S. revised it. M.K.K., F.I., B.L.B., and H.A.S. analyzed the data, and wrote the manuscript. All authors discussed and approved the results.

Flow locally washes away autoinducers and represses QS

To study QS dynamics under flow, we introduced *Staphylococcus aureus* into microfluidic devices[8] and continuously flowed sterile medium through the chambers with flow speeds comparable to those found in hosts[9,10]. The *S. aureus* strain harbored an *agr* P3-*gfpmut2* transcriptional fusion[11], which is activated in response to the endogenously produced QS autoinducer called AIP-I[2] (Supplementary Fig. 1a), and a constitutively expressed *sarA* P1-*mKate* transcriptional fusion[12], which enabled us to normalize measurements of QS responses by correcting for the effects of growth (Supplementary Fig. 1c and 1d).

S. aureus had a doubling time of 2.36 h in flow compared to 3.39 h in the absence of flow presumably because flow provided oxygen and nutrients (Fig. 1a). After 6 h, near the inlet, there were about three times more cells under flow than in the no-flow case. Nonetheless, high-cell-density dependent QS was only activated under the no-flow condition (Fig. 1b,c and Supplementary Video 1). We obtained identical result – no QS – under flow rates even as low as 0.5 μL/min, suggesting that flow effectively removes endogenously-produced autoinducers. Results similar to this have been reported previously[6,7,13]. To confirm this idea, QS autoinducers or autoinducer antagonists were exogenously introduced into the flow (Supplementary Fig. 2a) and, irrespective of the flow rate we used, QS was activated and repressed, respectively. Analogous results were obtained using the Gram-negative pathogen *Vibrio cholerae* (Supplementary Fig. 2b), suggesting, as has previous work[6,7], that this is a general phenomenon. QS represses biofilm formation in both *S. aureus* and *V. cholerae*, underscoring why robust biofilms form under flow[14–16] (Fig. 1c and Supplementary Fig. 2b).

QS can be expected to be repressed under sufficiently strong flow due to the advection of autoinducers. Considering the ubiquity of QS mechanisms in bacteria, we wondered if there exist realistic scenarios in which QS is activated even under flowing systems. The remainder of this work explores several examples of such responses and makes the case that more sophisticated assessment of the influence of flow, in conjunction with a consideration of geometry and surface topography, is required to capture and understand how such features drive non-uniform spatial and temporal dynamics of bacterial QS.

Forming a thick biofilm promotes QS under flow

We investigated whether *S. aureus* biofilm formation affects QS dynamics under constant flow. We found that QS was locally repressed for cells that were close to the flowing fluid, but QS was activated at the base of thick biofilms (Fig. 2a and 2b (i), and Supplementary Video 2). We interpret this result, highlighting the spatial distribution of QS, to mean that advection of autoinducers by flow is efficient at the interface between the biofilms and the flowing fluid[13,17,18], but is not efficient at the base[13,19], where autoinducers inside biofilms can accumulate, increasing in concentration over time.

To explore QS induction inside biofilms, we terminated the flow at 13 h, waited for an additional 3 h, during which diffusion was the only transport mechanism, and then examined the QS reporter output. Diffusion was less efficient than advection at removing autoinducers,

and QS activation indeed extended further into the inner region of the biofilm (Fig. 2b (ii)). If, by contrast, we maintained the flow for the entire 16 h, QS activation was restricted to the cells at the bottom of the biofilm (Supplementary Fig. 3). Under 100-fold higher flow speed, QS activation within the biofilm did not occur (Fig. 2c). The heterogeneous QS activation that occurs within biofilms under flow also depends on biofilm thickness. Under constant flow, increasing the biofilm thickness over a fixed area increases QS activation (Fig. 2d). Thus, the interplay between flow strength and biofilms leads to a spatially structured QS activation under flow.

Our findings could underscore a curious biofilm phenotype known for *S. aureus*. Activation of QS in *S. aureus* leads to upregulation of components that degrade the biofilm extracellular matrix[20,21] (Supplementary Fig. 1a), which is presumed to enable cells to escape, spread, and colonize new regions[22,23]. Our results show that cells that are in contact with flow are in QS-off mode, so they produce robust biofilms, which shield cells inside the biofilm from autoinducer advection. Presumably, this feature enables internal cells to be in the QS-on mode, to launch the gene expression program required for dispersal, facilitating flow-driven dissemination during infection.

In a separate set of experiments we also found that, regardless of biofilm thickness, intermittent flow promotes temporal fluctuations in and out of the QS-mode, ultimately leading to QS activation, albeit following an initial delay and only sub-maximal activation occurs (Supplementary Fig. 4). Thus, our studies suggest that time-varying flows that mimic rain, digestion, and urination can lead to non-uniform temporal QS activation.

QS responses vary as a function of distance to the flow inlet

Bacterial niches with connectivity over long distances are common in confined geometries, for example, bacterial contamination in piping, microbial distribution in soil, porous media, phloem in plants, or the intestinal tracts of animals. We wondered whether constant flow represses QS uniformly over long distances. To test this idea, we designed extended chambers with physiologically relevant length scales (~ 0.3 m). We found that QS is locally repressed by flow near the inlet, but in these confined environments, QS is activated downstream (Fig. 3a,b and Supplementary Video 3). Relatively more biofilm formation was observed in the upstream region than downstream at later time points presumably due to the consequences of QS-driven differences in biofilm regulation. As fluid travels over a surface colonized by bacteria that produce autoinducers, the average autoinducer concentration in the flowing fluid increases downstream over time. We changed the flow speeds to examine if QS activation was affected. The autoinducer concentration at distance x is approximately proportional to the travel time t of flowing fluid ($t \propto x/Q_{\text{fluid}}$). As we increase the flow rate Q_{fluid}, the travel time to distance x decreases so the autoinducer concentration at distance x decreases. Thus, as flow rate increases, the critical distance D_c to initiate QS activation increases (Supplementary Fig. 5a).

To understand how autoinducer concentration increases as fluid travels downstream, we developed a mathematical model of the kinetics and convection (see Supplementary equations). The model predicts the concentration profiles as a function of distance and time,

showing accumulation downstream, which promotes specific regions in which QS is induced (Fig. 3c and Supplementary Fig. 5b). Our findings suggest that, compared with the no-flow scenario in which QS-mediated communication is driven exclusively by diffusion, the transport of autoinducers by flow in confined configurations increases the length scale of bacterial communication so that QS-directed processes are non-uniform along natural flow pathways. This finding might explain why *Pseudomonas aeruginosa* is motile upstream (a QS-off phenotype), but forms biofilms downstream (a QS-on phenotype) in flowing networks[24].

QS is activated in crevices despite flow

Next we considered whether complex topographies (grooves, crevices, pores) might also influence QS-mediated communication. Crevices such as cracks in rocks, tooth cavities, intestinal crypts, and corrugated pipes are a few examples where bacterial colonization can occur (Fig. 4a). In the present context, *S. aureus* colonizes human intestinal crypts and this behavior is central to its pathogenic lifestyle[25]. We designed chambers with crevices, and initially examined flow patterns by imaging particles in the fluid (Fig. 4b). Outside the crevices, particles moved with the flow with convection being the dominant feature (flow-dominant region), while inside the crevices, the tracer particles remained at rest and diffusion dominated (flow-limited region)[26]. When we seeded bacteria into the chamber, QS was repressed outside the crevices, similar to what we found under constant flow (Fig. 1). However, QS was activated inside the crevices (Fig. 4c and Supplementary Video 4). The results show that autoinducer accumulates inside crevices as a result of the reduction of flow, which depends on the aspect ratio of the cavities, L_c/W_c. In crevices with low L_c/W_c, in which flow can penetrate and advection is dominant, autoinducers were washed away, and QS was repressed (Supplementary Fig. 6a).

Our findings could underscore a pathogenic behavior of *S. aureus*. Inside crypts, *S. aureus* engages in QS and activates the production of enterotoxin B, which functions to increase the depth of the crypt[3,27]. According to our findings, this activity further insulates *S. aureus* from flow, which is a mechanism that presumably enables QS-control of pathogenicity specifically inside crypts (Fig. 4c). The consequences of topography are apparently generalizable: the Gram-negative enteric pathogen *V. cholerae*, which also colonizes human intestines and uses QS to control virulence[28,29], also activates QS inside, but not outside, crevices (Supplementary Fig. 6b).

To explore the health consequences of QS in complex topographies, we introduced into the flow a molecule that acts as an antagonist (AIP-II) of the *S. aureus* autoinducer[30]. In response to antagonist diffusion into crevices, QS was repressed (Fig. 4d). Analogous results were obtained using the clinical pathogen *S. aureus* MRSA (Supplementary Fig. 6c,d and Supplementary Video 5), which highlights the generality of our results and approach.

We have discovered unexpected QS dynamics under different flow regimes, which arise from the interactions between bacterial signaling pathways, small molecule diffusion, convection, the geometry and thickness of the biofilms, the length of the diffusive path within cell clusters, and the distances and topographies characteristic of flow networks.

These findings enable us to predict how QS will play out in different spatio-temporal contexts which will have significant implications for the development of strategies for controlling beneficial and pathogenic bacterial behaviors in realistic environments in nature, in medicine and in industry. Our results specifically suggest that bacterial colonization and biofilm development under flow can lead to heterogeneous QS activation (Supplementary Fig. 7), which promotes diversity in the genetic programs that bacteria enact. As a consequence, genetically identical bacteria exhibit remarkably different behaviors at particular regions and at particular times under flow.

Methods

Bacterial strains, plasmids, and autoinducer peptides

The strains and plasmids used are listed in Supplementary Table 1. *Staphylococcus aureus* strains RN4220 and RN6390b, and the plasmid pJL-agr-GFP were gifts from Dr. Richard Novick's group (New York University)[10]. DNA polymerase, dNTPs, and restriction enzymes were purchased from New England Biolabs (NEB, Ipswich, MA). DNA extraction and purification kits were acquired from Qiagen (Valencia, CA). DNA oligonucleotides were purchased from Integrated DNA Technologies (Coralville, Iowa). Sequences of plasmids were verified by Genewiz (South Plainfield, NJ). The autoinducer AIP-I and the autoinducer antagonist AIP-II were synthesized as previously described[30], using standard solid-phase approaches.

A plasmid carrying a transcriptional fusion to monitor *S. aureus* QS activity was constructed by replacing the *gfpmut2* gene from vector pJL-agr-GFP with a fragment containing *agr* P3-*mKate*. This plasmid is called pMK004. To make this plasmid, the *mKate* gene was amplified by PCR from pCN004[31] using primers MKF012/MKR012 followed by overlap extension PCR cloning[32]. A plasmid constitutively expressing mKate under the *sarA* P1 promotor (pMK014), was constructed by replacing the *agr* P3 promoter in pMK004 with the constitutive promoter *sarA* P1. The *sarA* P1 sequence corresponded to −306 to −62 upstream of *sarA*, and was amplified from *S. aureus* RN6390b using primers MKF001/MKR001[10,11,33], followed by overlap extension PCR cloning. The final plasmid harboring both the *agr* P3-*gfpmut2* and the *sarA* P1-*mKate* fusions (pMK021) was constructed by introducing the *sarA* P1-*mKate* fragment onto pJL-agr-GFP using Gibson cloning (New England Biolabs, Ipswich, MA)[34]. All plasmids were introduced into *Escherichia coli* DH5α using chemical transformation (New England Biolabs, Ipswich, MA) followed by selection with ampicillin. Vectors were purified from *E. coli*, introduced into *S. aureus* strain RN4220 by electroporation, and selected with erythromycin[35]. Subsequently, vectors were transduced into *S. aureus* strain RN6390b or the MRSA strain using standard phage transduction techniques with phage 80α[35].

Growth conditions

S. aureus strains were grown overnight at 37 °C with shaking in Tryptic Soy Broth (TSB; Difco, Franklin Lakes, NJ) with 10 μg/ml erythromycin to maintain plasmids, back-diluted 1:2000, and re-grown for 3 h (to OD_{600} ~ 0.05–0.1). *V. cholerae* strains were grown

overnight at 37 °C with shaking in Tryptone Broth (TB; Difco, Franklin Lakes, NJ), back-diluted 1:1000, and re-grown for 3 h to early exponential phase.

Fluorescence reporter assay

Transcription from fluorescence reporter genes was measured in *S. aureus* strain RN6390b carrying pMK021 (MK121). Overnight *S. aureus* cultures were diluted 1:1000 into fresh TSB with 10 μg/ml erythromycin, and 100 μL of diluted cultures were distributed into wells of 96 well plates (MatTek, Ashland, MA), followed by addition of 50 μL of mineral oil (Sigma, St. Louis, MO) to prevent evaporation. Using a Synergy 2 plate reader (Biotek, Winooski, VT), OD_{600} was monitored, and GFP and mKate levels were measured at 484 nm/528 nm and 588 nm/633 nm, respectively. Measurements were conducted with 15 min intervals at 25 °C with shaking.

Microscopy

Imaging was performed using a Nikon Eclipse Ti microscope (Melville, NY) fitted with a Yokogawa CSU X-1 spinning disk confocal scanning unit (Biovision Technologies, Exton, PA), CFI Apo TIRF 60X Oil objective (Nikon, Melville, NY), and DU-897 X-9351 camera (Andor, Concord, MA). Laser lines at 488 and 593 nm were used to excite the GFP and mKate fluorescent proteins, respectively. We imaged the surface area of 400 μm × 500 μm, 250 μm × 250 μm, 125 μm × 250 μm, and 750 μm × 625 μm for Fig. 1, 2, 3 and 4, respectively. For Fig. 1, 2, and 4, images were taken at the bottom of the channels. Cell counts and quantitation of QS output were processed using custom software written in Matlab (Mathworks, Natick, MA). Fluorescence protein signals were distinguished from background noise by subtraction of background signals. To calculate cell counts, the constitutive mKate fluorescence from the total imaged bacterial biomass area was summed and divided by the experimentally determined average fluorescence signal of single cells. Normalized QS output is defined as the normalized GFP intensity, which was obtained by summing the QS-controlled GFP fluorescence intensity from the total imaged bacterial biomass area followed by subtraction of background noise and division by the cell counts. Each replicate was performed using independent bacterial cultures in individual chambers. For experiments exploring crevice geometries, we measured fluorescence intensities from three crevices and combined the data to become a single replicate. All experiments were conducted at room temperature.

Microfluidic experiments

Details of fabrication and experiments are provided in supplementary information. Channels were loaded with cultures for 10 min, after which sterile TSB containing 10 μg/ml erythromycin was flowed steadily into the devices to remove unattached planktonic cells. The flow into the main channel was constant or periodic with a range of Q_{fluid} = 0.1–100 μL/min. The flow was driven by syringe pumps. For *V. cholerae* experiments, sterile TB was used as the medium.

Supplementary Material

Refer to Web version on PubMed Central for supplementary material.

Acknowledgments

We thank the Novick laboratory for generously providing *S. aureus* strains and the pJL-agr-GFP plasmid. We thank B. Wang, J. Chen, K. Papenfort and J. Yan for technical advice and discussions, and we thank K. Drescher for discussions and for generously providing strain KDV028. We thank A. Ismail for providing the image that appears in Fig. 4a (i) and W. Lee for the image in Fig. 4a (ii). We are grateful to members of the B.L.B. and H.A.S. laboratories for suggestions. This work was supported by NSF grant MCB-1119232 (B.L.B. and H.A.S.) and MCB-1344191 (B.L.B. and H.A.S), the Howard Hughes Medical Institute (B.L.B.), NIH grant R01GM065859 (B.L.B.), and STX fellowship (M.K.K.).

References

1. Bassler BL, Losick R. Bacterially speaking. Cell. 2006; 125:237–246. [PubMed: 16630813]
2. Novick RP, Geisinger E. Quorum sensing in staphylococci. Annual Review of Genetics. 2008; 42:541–564.
3. Arvidson S, Tegmark K. Regulation of virulence determinants in *Staphylococcus aureus*. International Journal of Medical Microbiology. 2001; 291:159–170.
4. Persat A, et al. The mechanical world of bacteria. Cell. 2015; 161:988–997. [PubMed: 26000479]
5. Purevdorj B, Costerton JW, Stoodley P. Influence of hydrodynamics and cell signaling on the structure and behavior of *Pseudomonas aeruginosa* biofilms. Applied and Environmental Microbiology. 2002; 68:4457–4464. [PubMed: 12200300]
6. Kirisits MJ, et al. Influence of the hydrodynamic environment on quorum sensing in *Pseudomonas aeruginosa* biofilms. Journal of Bacteriology. 2007; 189:8357–8360. [PubMed: 17704224]
7. Meyer A, et al. Dynamics of AHL mediated quorum sensing under flow and non-flow conditions. Physical Biology. 2012; 9:026007. [PubMed: 22476057]
8. Rusconi R, Garren M, Stocker R. Microfluidics expanding the frontiers of microbial ecology. Annual Review of Biophysics, Vol 43. 2014; 43:65–91.
9. Fine KD, Santaana CA, Porter JL, Fordtran JS. Effect of changing intestinal flow rate on a measurement of intestinal permeability. Gastroenterology. 1995; 108:983–989. [PubMed: 7698614]
10. Lipowsky HH, Kovalcheck S, Zweifach BW. Distribution of blood rheological parameters in microvasculature of cat mesentery. Circulation Research. 1978; 43:738–749. [PubMed: 709740]
11. Liese J, Rooijakkers SHM, van Strijp JAG, Novick RP, Dustin ML. Intravital two-photon microscopy of host-pathogen interactions in a mouse model of *Staphylococcus aureus* skin abscess formation. Cellular Microbiology. 2013; 15:891–909. [PubMed: 23217115]
12. Cheung AL, Nishina K, Manna AC. SarA of *Staphylococcus aureus* binds to the *sarA* promoter to regulate gene expression. Journal of Bacteriology. 2008; 190:2239–2243. [PubMed: 18178734]
13. Stewart PS. Mini-review: Convection around biofilms. Biofouling. 2012; 28:187–198.
14. Weaver WM, Milisavljevic V, Miller JF, Di Carlo D. Fluid flow induces biofilm formation in *Staphylococcus epidermidis* polysaccharide intracellular adhesin-positive clinical isolates. Applied and Environmental Microbiology. 2012; 78:5890–5896. [PubMed: 22706049]
15. Kim MK, Drescher K, Pak OS, Bassler BL, Stone HA. Filaments in curved streamlines: rapid formation of *Staphylococcus aureus* biofilm streamers. New Journal of Physics. 2014; 16:065024.
16. Drescher K, Shen Y, Bassler BL, Stone HA. Biofilm streamers cause catastrophic disruption of flow with consequences for environmental and medical systems. Proceedings of the National Academy of Sciences of the United States of America. 2013; 110:4345–4350. [PubMed: 23401501]
17. Drescher K, Nadell CD, Stone HA, Wingreen NS, Bassler BL. Solutions to the public goods dilemma in bacterial biofilms. Current Biology. 2014; 24:50–55. [PubMed: 24332540]
18. Horswill AR, Stoodley P, Stewart PS, Parsek MR. The effect of the chemical, biological, and physical environment on quorum sensing in structured microbial communities. Analytical and Bioanalytical Chemistry. 2007; 387:371–380.
19. Stoodley P, Debeer D, Lewandowski Z. Liquid flow in biofilm systems. Applied and Environmental Microbiology. 1994; 60:2711–2716. [PubMed: 16349345]

20. Boles BR, Horswill AR. *agr*-mediated dispersal of *Staphylococcus aureus* biofilms. Plos Pathogens. 2008; 4:e1000052. [PubMed: 18437240]
21. Periasamy S, et al. How *Staphylococcus aureus* biofilms develop their characteristic structure. Proceedings of the National Academy of Sciences of the United States of America. 2012; 109:1281–1286. [PubMed: 22232686]
22. Yarwood JM, Bartels DJ, Volper EM, Greenberg EP. Quorum sensing in *Staphylococcus aureus* biofilms. Journal of Bacteriology. 2004; 186:1838–1850.
23. Parsek MR, Greenberg EP. Sociomicrobiology: the connections between quorum sensing and biofilms. Trends in Microbiology. 2005; 13:27–33.
24. Siryaporn A, Kim MK, Shen Y, Stone HA, Gitai Z. Colonization, competition, and dispersal of pathogens in fluid flow networks. Current Biology. 2015; 25:1201–1207.
25. Acton DS, Plat-Sinnige MJT, van Wamel W, de Groot N, van Belkum A. Intestinal carriage of *Staphylococcus aureus*: how does its frequency compare with that of nasal carriage and what is its clinical impact? European Journal of Clinical Microbiology & Infectious Diseases. 2009; 28:115–127. [PubMed: 18688664]
26. Pan F, Acrivos A. Steady flows in rectangular cavities. Journal of Fluid Mechanics. 1967; 28:643.
27. Benjamin MA, Lu J, Donnelly G, Dureja P, McKay DM. Changes in murine jejunal morphology evoked by the bacterial superantigen *Staphylococcus aureus* enterotoxin B are mediated by CD4(+) T cells. Infection and Immunity. 1998; 66:2193–2199.
28. Millet YA, et al. Insights into *Vibrio cholerae* intestinal colonization from monitoring fluorescently labeled bacteria. PLoS Pathogens. 2014; 10:e1004405. [PubMed: 25275396]
29. Zhao XA, Koestler BJ, Waters CM, Hammer BK. Post-transcriptional activation of a diguanylate cyclase by quorum sensing small RNAs promotes biofilm formation in *Vibrio cholerae*. Molecular Microbiology. 2013; 89:989–1002. [PubMed: 23841714]
30. George EA, Novick RP, Muir TW. Cyclic peptide inhibitors of staphylococcal virulence prepared by Fmoc-based thiolactone peptide synthesis. Journal of the American Chemical Society. 2008; 130:4914–4924. [PubMed: 18335939]

Additional References

31. Nadell CD, Bassler BL. A fitness trade-off between local competition and dispersal in *Vibrio cholerae* biofilms. Proceedings of the National Academy of Sciences of the United States of America. 2011; 108:14181–14185. [PubMed: 21825170]
32. Bryksin AV, Matsumura I. Overlap extension PCR cloning: a simple and reliable way to create recombinant plasmids. Biotechniques. 2010; 48:463–465. [PubMed: 20569222]
33. Malone CL, et al. Fluorescent reporters for *Staphylococcus aureus*. Journal of Microbiological Methods. 2009; 77:251–260. [PubMed: 19264102]
34. Gibson DG, et al. Enzymatic assembly of DNA molecules up to several hundred kilobases. Nature Methods. 2009; 6 343-U41.
35. Novick RP. Genetic Systems in Staphylococci. Methods in Enzymology. 1991; 204:587–636. [PubMed: 1658572]

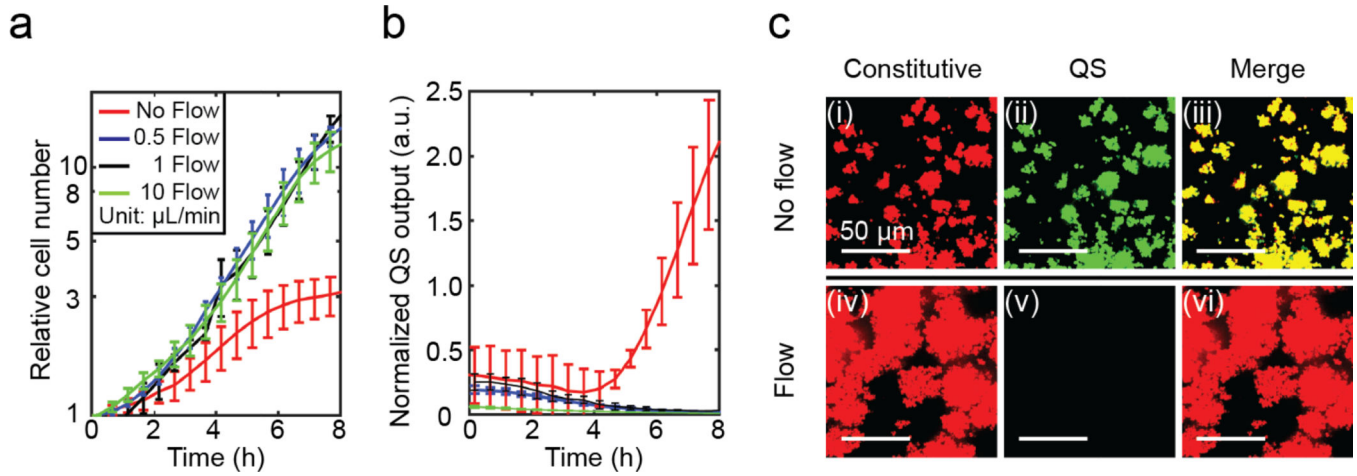

Figure 1. Fluid flows locally repress QS by advecting signaling molecules

a, (i) Growth curves obtained by measuring mKate fluorescence intensity from the *S. aureus sarA* P1-*mKate* reporter under different flow conditions; flow rates of 0–10 μL/min. Relative cell number denotes the number of cells divided by the initial cell number. Cell counts were obtained as dividing the summed mKate fluorescence intensity by the experimentally determined average fluorescence signal of individual cells. (ii) Normalized QS output is the GFP fluorescence intensity from the QS-controlled *agr* P3-*gfpmut2* reporter divided by the cell counts as a function of time for different flow conditions. We imaged the surface area of 400 μm × 500 μm, which is one quarter of the area of the channel. Data points indicate means and error bars denote standard deviations with n = 4 independent replicates. **b**, Fluorescence images of *S. aureus* under no flow and flow conditions 6 h after inoculation. Left panels (i) and (iv) show the constitutive *sarA* P1-*mKate* reporter. Middle panels (ii) and (v) show the QS-controlled *agr* P3-*gfpmut2* reporter. Right two panels (iii) and (vi) show the merged images for the left and middle panels. Top panels (i), (ii), and (iii); no flow, bottom panels (iv), (v), and (vi); flow rate of 1 μL/min. The images are based on n = 4 independent replicates.

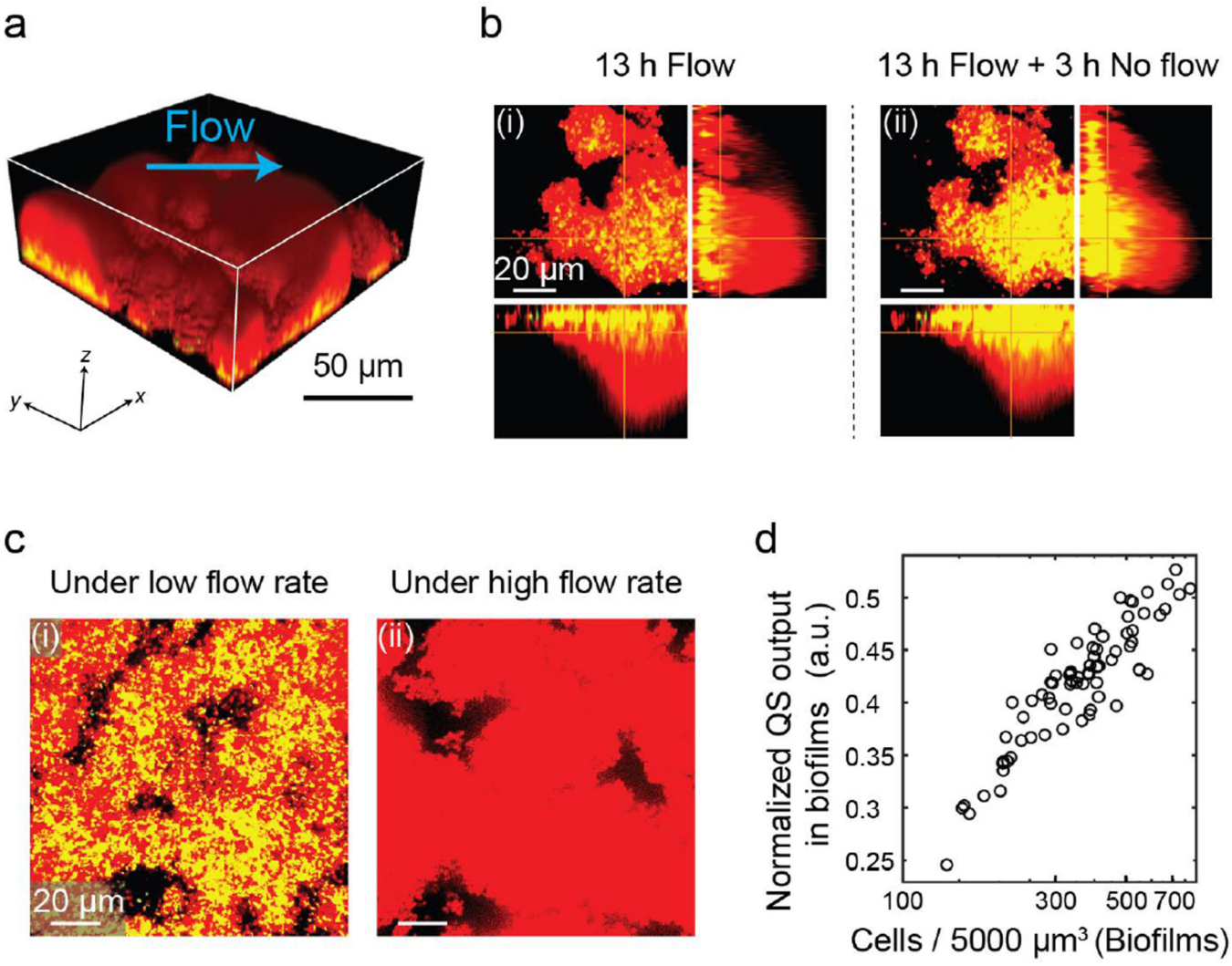

Figure 2. Forming a thick biofilm promotes QS under flow

a, A three-dimensional rendering of biofilms (127 μm × 127 μm × 50 μm) of *S. aureus* grown in a microfluidic channel (Q_{fluid} = 0.1 μl/min). The figure is the merged image (see Fig. 1 for details); red indicates QS-off cells, and yellow indicates QS-on cells. The images are based on n = 4 independent replicates. **b**, Central merged images show single optical sections of the xy plane, 10 μm above the surface-biofilm interface, with z-projections shown at right (xz plane) and below (yz plane). The same biofilm region is shown (i) under flow for 13 h after inoculation and (ii) following 13 h of flow and 3 h of no flow. The images are based on n = 4 independent replicates. **c**, Merged images for the base of biofilms grown under different flow rates, (i) 0.1 μL/min and (ii) 10 μL/min, were taken 13 h after inoculation. The images are based on n = 4 independent replicates. **d**, Normalized QS output was measured as a function of cell number in a volume of 5000 μm^3 (100 μm^2 area × 50 μm height).

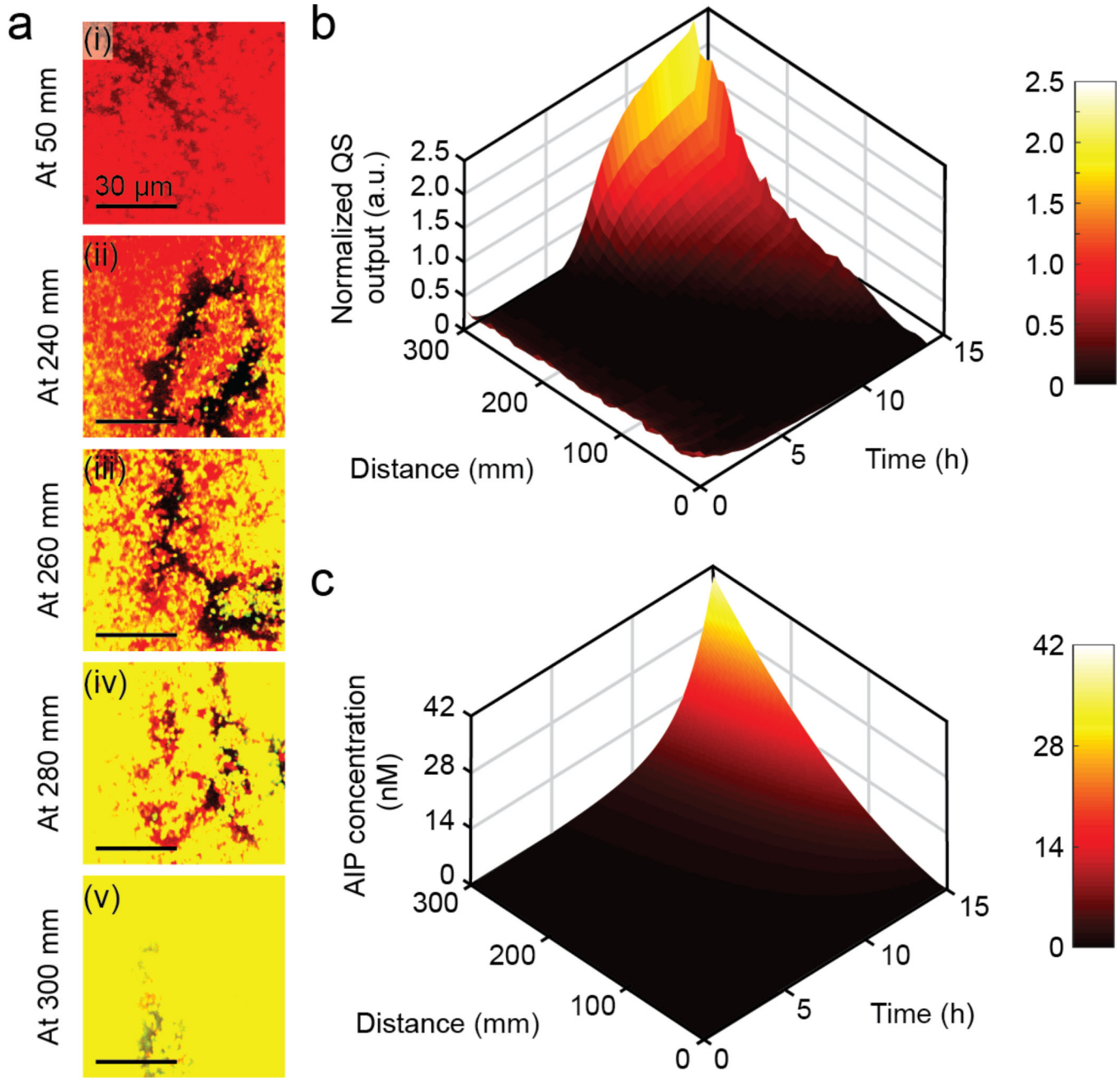

Figure 3. Flows assist long-distance QS by enhancing autoinducer accumulation

a, Merged images (see Fig. 1 for details) at different downstream locations along a microfluidic channel (Q_{fluid} = 0.5 μl/min): (i) 50 mm, (ii) 240 mm, (iii) 260 mm, (iv) 280 mm and (v) 300 mm 14 h after the start of the experiment. The images are based on n = 3 independent replicates. **b**, Spatio-temporal evolution of the normalized QS output (Q_{fluid} = 0.5 μl/min). Data indicate means of normalized QS output for triplicate data. **c**, Model prediction for the autoinducer concentration profile as a function of space and time (see Supplementary Equations).

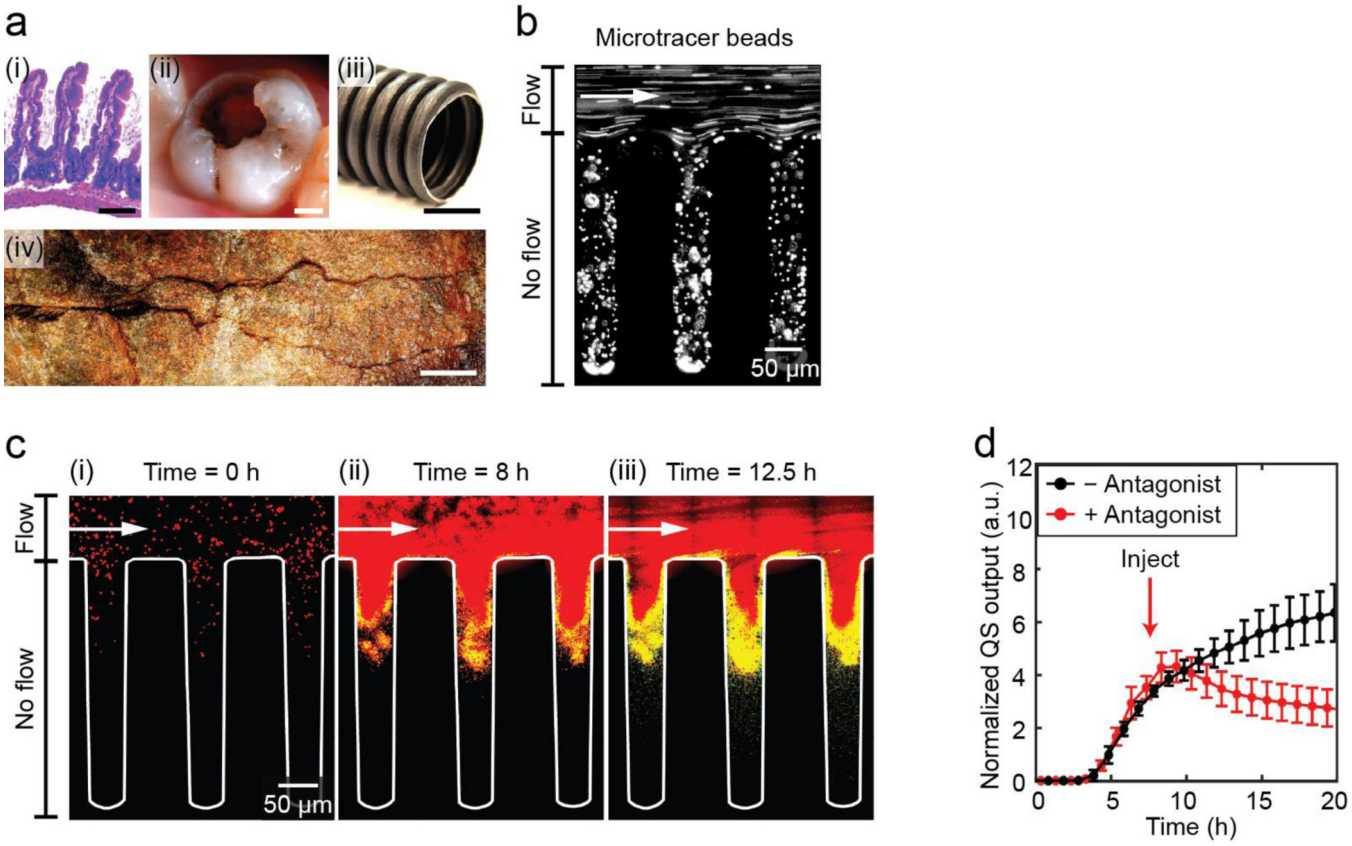

Figure 4. QS is activated inside crevices

a, Flow networks with crevices or pores in (i) the small intestine of mice (image courtesy of Dr. Anisa Ismail), (ii) tooth cavities (image courtesy of Dr. Wonhee Lee), (iii) corrugated industrial pipes, and (iv) cracks in rocks. Scale bars: 120 μm, 10 mm, 2 cm, and 5 cm, respectively. **b**, Image of fluorescent 1 μm diameter beads flowing into a corrugated microfluidic channel under a flow rate of 1 μL/min. The images based on n = 4 independent replicates. **c**, Merged images of *S. aureus* in a complex topography. As in Fig. 1, red shows QS-off cells, and yellow shows QS-on cells. The images are based on n = 6 independent replicates. **d**, Normalized QS output inside of crevices in the absence of antagonist (black) and when 1 μM antagonist (AIP-II) was continuously flowed in beginning 8 h after inoculation (red). Data points indicate means and error bars denote standard deviations with n = 4 independent experiments.